3D finite element analysis of wheel-rail profiles in different contact conditions

Mehdi Darvishi[1], Mahnoosh Ghaderi[2], Roya Sadat Ashofteh[3,] Amin Owhadi[4*]

[1]M.sc of Rolling Stocks, Faculty of Railway Engineering, Iran University of Science and Technology.

[2]B.sc of Rolling Stocks, Faculty of Railway Engineering, Iran University of Science and Technology.

[3]Raja railway transportation Co.

[4]A. Professor, Faculty of Railway Engineering, Iran University of Science and Technology, Tehran, Iran.

ARTICLE INFO	A B S T R A C T
	In the field of wheel-rail contact, many researches have been done into rolling profiles in this paper, three wheels from passenger wagons and two standard rails UIC60 and U33 are considered. The calculation of contact parameters including contact surface dimensions, stress, and pressure makes it possible to investigate wheel and rail profile conformity in different contact conditions including straight track, curving, and crossing. Hertz contact method and finite element analysis were used for this purpose. The comparison of mentioned parameters for six pairs of wheel and rail was conducted. The results show that in the case of straight track and curving wheel III has smaller contact stresses and pressures but in the case of crossing wheel I represents an acceptable performance in contact with rail UIC60. Taken together, the results indicate a weak performance of rail U33 in all cases.

1. Introduction

With the recent increase in railway operating speed and load, a great number of studies have focused on the contact between wheel and rail. The selection of a wheel rolling profile has always been one of the challenges facing engineers. Wheels with conical profiles improve vehicle performance, especially in curving. Based on observed wear patterns, wheel profile shapes become more complex to achieve longer periods between wheel re-profilings [1]. Modification of standard wheel and rail profiles to adapt to specified operating conditions and minimize fatigue and wear has been a long-standing effort by researchers. In most cases, the goals are profile matching and single-point contact [2]. Wheel and rail profiles should correspond to each other and due to this reason,

the conformity of wheel and rail surfaces is a challenging area in the field of wheel/ rail contact [3], [4].

Wheel and rail profiles have received considerable attention over the years and a great number of research papers have been published on this topic. In the field of wear study, J. Auciello et al. [5] represented the undeniable effect of wheel profile shape on vehicle dynamic and stability performance in both straight and curved tracks.

Wu et al. [6] investigated the influence of operating conditions including wheel profile on wheel wear. They claim that wheel wear is strongly influenced by proper wheel profile selection and equivalent conicity.

Jia-Huan et al. [7] developed a finite element method to compare the performance of four

---

*Corresponding author
Email address: aohadi@iust.ac.ir

different wheel profiles with standard 60-profile rail under various working conditions such as axle load and traction. This comparison is made by considering the size of the contact area, equivalent stress, and contact force. The results of this study indicated that wheel I has better matching performance.

Esen et al. [8] adopted ANSYS software to simulate the interaction of the UIC60 rail profile and UIC515 wheel profile in different positions of the wheel over the sleeper. Comparative results of stress distributions in contact point and plastic deformations on the rail and wheel represented lower stress in the wheel's position over the sleeper and lower elastic strain in the wheel's position between two sleepers.

Özdemir et al. [9] presented a FE model of the UIC60 rail and S1002 wheel profile, considering the wheel and rail material behavior effect on the result of pressure level and contact area. The findings of this study indicate that applying elastic/ plastic material assumptions affects the output of the contact interface.

Gurubaran et al. [10] carried out a three-dimensional FEA to identify the maximum stress concentration in the wheel-rail contact zone and compare it with the wheel and rail steel yield stress limit to specify the initial damage growth area.

Since the Hertz Theory was published, it has been applied considerably in various engineering subjects, especially wheel and rail contact.

Sharma et al. [11] used Quasi–Hertz and carried out FE analysis of rail UIC60 and a standard wheel profile to study the influence of wheel and rail profile interaction on stress distribution and contact zones.

Results of different methods, including the Hertz method compared by Lack et al. [12] to investigate the effect of wheel and rail profile shapes on the size of the contact area and normal stress over this area. The results of the investigation demonstrate a significant effect of wheel and rail shapes on contact area in all aspects such as shape and stress distribution.

To develop a new profile design, Srivastava et al [13] utilized the results of the FEM and Hertz's approach in contact geometry and stress distribution.

Sladkowski et al. [14] used mathematical simulation based on both the quasi-Hertz method and finite element (FE) method to investigate the effect of wheel and rail profiles interaction on stresses and distribution of contact zones. The results of this study developed the required basis for designing new wheel and rail profiles.

The present paper aims to study the contact between three different wheels and the most widely used rail in Iran's railway network. In this content, finite element models of wheel and rail are implemented in ABAQUS 6.14 software. The results of the contact need to be validated. For this purpose, the Hertz theory is chosen.

2. Materials

The approved and widely used rails in Iran railway are UIC60 and U33, which are equivalent to 60EI and 46E2 in European norms respectively. EN13674 states the mechanical characteristics and geometric parameters of rails [15]. On the subject of the wheels, EN13262 reported the mechanical properties of ER8 steel grade [16]. Figures 1 to 5 present details of wheel and rail profiles.

3. Modelling/ FEM

To analyze wheel and rail contact conditions and calculate stresses and pressures in the contact area, finite element software ABAQUS is set up.

FEM/ FEA is one of the most common problem-solving methods in the field of mechanical engineering based on computer numerical techniques. In this analysis, the wheel and rail rigid structures are divided into finite numbers of elements called mesh.
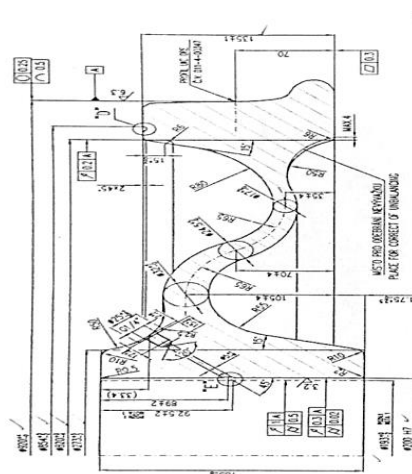

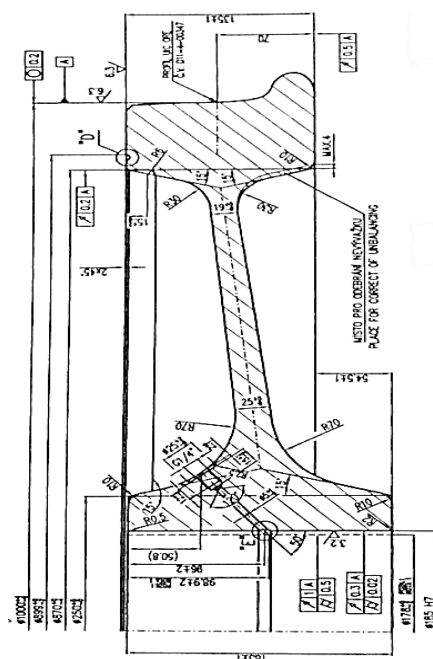Figure 1. wheel I
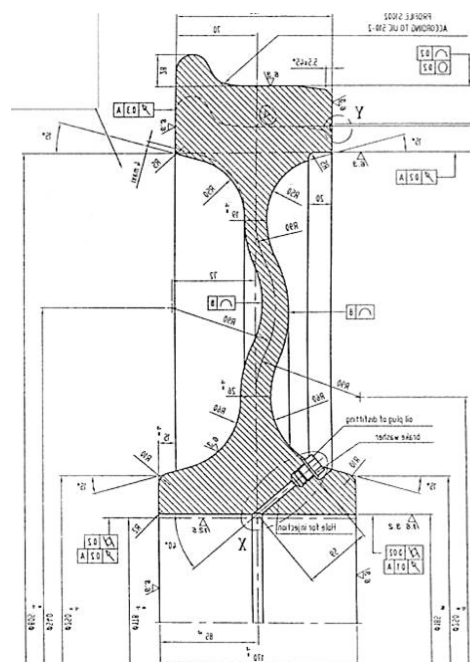
Figure 2. wheel II

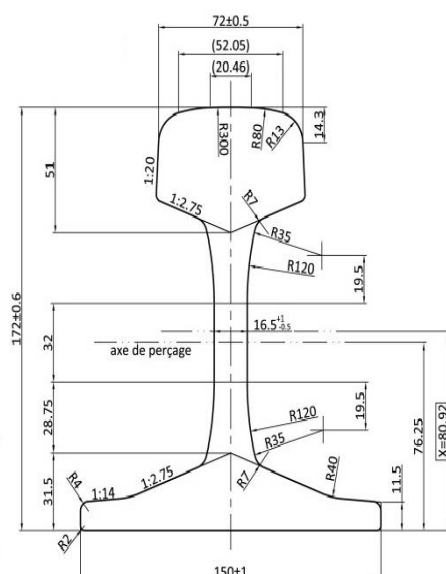

Figure 3. wheel III

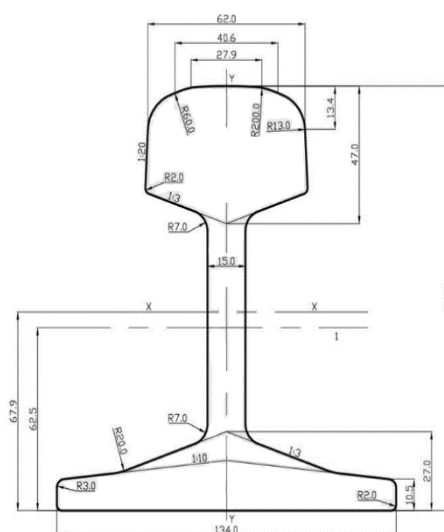Figure 4. Rail profile UIC60

Figure 5. Rail profile U33

The analysis can simulate wheel and rail behavior in the contact area by considering the material's characteristics and behavior. Contact stresses and pressures, stress distribution, contact patch size, etc. can be determined as analysis results. The approach to contact geometry and stress distribution.

3.1. Loading

In this study, wheel and rail are considered rigid bodies, and the contact is established at one point called the 'contact point' [17]. Wheel and rail contact conditions, including the number and position of contact points, can be very important in terms of their remarkable effect on wear and

dynamic performance [18]. The applied vertical load in wheel-rail contact was presented $P = 73500N$. Railway standard EN 13979 defines load P as half of the vertical force per axle on the rail [19]. This value is associated with the vehicle's (a passenger wagon) total weight, about 60 Tons, assuming that the wagon has four axles.

According to the mentioned standard, loading should be done by considering three different cases due to the track conditions including straight track, curves, and crossing. In case 1, straight track, the wheelset is in the centered position. In case 2, curves, the wheel flange is pressed against the rail and in case 3, crossings, the inside surface of the wheel flange is in contact with the rail.

The position and number of applied loads for each case based on P load are specified respectively in Figure 6 and Table 1.

Table 1. Number of loads for each case

	F_z	F_{y2}	F_{y3}
Case 1	1.25 P		
Case 2	1.25 P	0.6 P	
Case 3	1.25 P		0.36P

3.2. Boundary conditions

Implementation of boundary conditions is an essential step after finite element model completion. These conditions represent model constraints and motion restrictions. Actual material properties, fine meshing structure, real constraints, and boundary conditions significantly improve analysis accuracy [8]. Rail movement in the vertical direction is restricted by using the fixed type of constraint at the bottom of the rail.

The conical shape of the wheel profile brings unwanted motion in the lateral direction during simulation [9]. To simplify the analysis procedure, it is assumed that the movement of the wheel is limited only in the longitudinal direction.

The constraints, boundary conditions, and rail and wheel degrees of freedom were defined as shown in Figure 7.
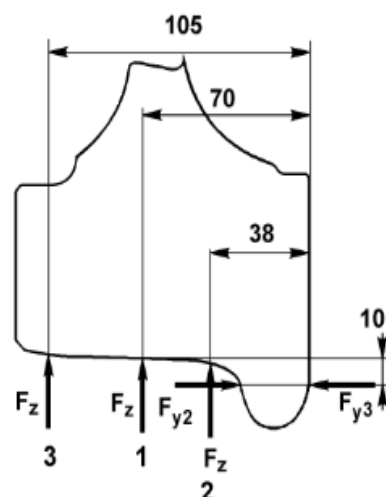

Figure 6. Position of loads for each case

3.3. Meshing

Due to the number of stresses and strains on the wheel and rail contact area and consequently the high accuracy requirement, the fine mesh must be implemented in the upper part of the rail and lower part of the wheel [20]. Several elements and nodes for the modeled rails and wheels, described in the FE meshed model, are listed in Table 2. Therefore, the hole model consists of at least 18076 elements and 29341 nodes.
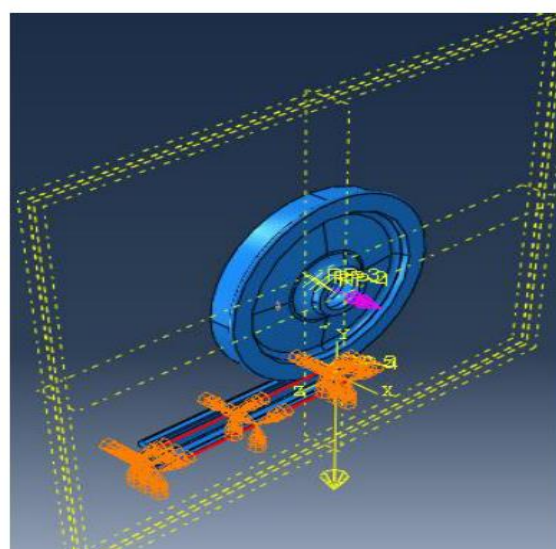

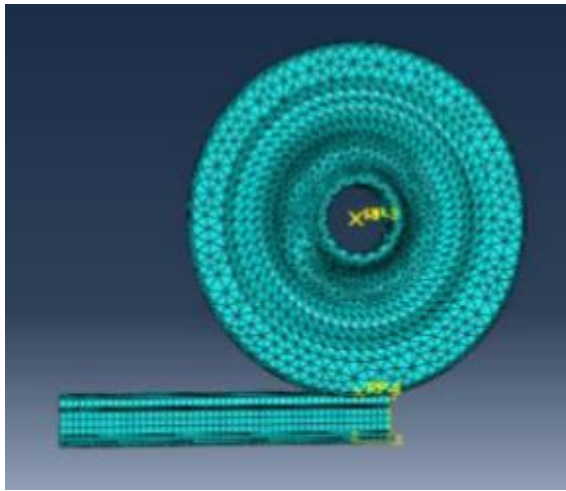Figure 7. Applied boundary conditions

Figure 8. The meshing of the wheel and the rail

Table 2. Number of wheels and rail elements and nodes

	RailUIC60	RailU33	Wheel1	Wheel2	Wheel3
Elements	5160	4850	13217	14812	18868
Nodes	7015	6324	23017	24750	32227

4. Hertz Theory: (The validation of FEM results)

Contact surface, pressures, and forces are defined as the contact parameters that must be determined in the first step of solving the contact problems [17]. The Hertz approach is then developed to validate normal contact dimensions and pressures. Hertz claims that if two elastic bodies were pressed together with a normal force, the contact surface and contact pressure can be calculated by considering particular assumptions.

According to the Hertz theory, the contact geometry is considered elliptical with a semi-major axis 'a' and a semi-minor axis 'b' as shown in Figure 9. R_{11}, R_{12}, R_{21} and R_{22} are defined as the rolling radius of curvature of the wheel, the radius of the wheel profile, the radius of the runway, and the radius of curvature of the rail respectively.

The radius of wheels used in this study varies from $R_{11} = 460$ and 500 mm and the wheel transverse radius is $R_{12} = 330$ mm (according to the curvatures radii of S1002 wheel profile) whereas R_{21} is infinite.
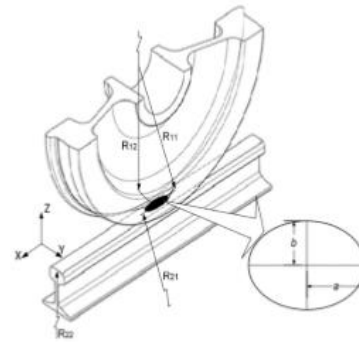

Figure 9. wheel-rail elliptical contact

$$A = \frac{1}{2} \times \frac{1}{R_{11}} = \frac{1}{2} \times \frac{1}{460 \times 10^{-3}} = 1.0869 \quad (1)$$

$$B = \frac{1}{2} \times \left(\frac{1}{R_{12}}\right)$$

$$= \qquad\qquad (2)\frac{1}{2}$$

$$\times (\frac{1}{330 \times 10^{-3}}) = 1.6666$$

(Deduced from the transverse profiles)

$$a = m\left(\frac{3}{2}N\frac{1-\nu^2}{E}\frac{1}{A+B}\right)^{1/3} = \qquad (3)$$

$$1.128 \times \left(\frac{3}{2} \times 91875 \times \frac{1-0.3^2}{205\times10^9} \times \frac{1}{2.7535}\right)^{1/3}$$

$$= 6.8318 \times 10^{-3}m = 6.8313 \; mm$$

$$b = n\left(\frac{3}{2}N\frac{1-\nu^2}{E}\frac{1}{A+B}\right)^{1/3} \qquad (4)$$

$$= 5.4067 \; mm$$

The constants values m and n in the formulae depend on the angle θ, which is given in Table 3.

$$\cos\theta = \frac{|B-A|}{A+B} \qquad (5)$$

$$\theta = \cos^{-1}\left(\frac{|B-A|}{A+B}\right) = 77.84° \qquad (6)$$

The Young's modulus E= 205 GPa and the Poissons ratio $\nu = 0.3$ are the mechanical properties of material assumed to be same for

wheel and rail in Hertzian calculation. The contact load is 91875 N.

Table 3. Hertz Coefficients ((A/B) <1)

θ°	90	80	70	60	10	0
g = n/m	1	0.7916	0.6225	0.4828	0.0470	0
m	1	1.128	1.285	1.486	6.612	∞
n	1	0.8927	0.8000	0.7171	0.3110	0
r	1	0.9932	0.9726	0.9376	0.4280	0

The maximum pressure in elliptical pressure distribution can be calculated as follows:

$$\sigma_{max} = \frac{3}{2}N\Big/\pi ab = \qquad (7)$$

$$\frac{3 \times 91875}{2 \times \pi \times 6.8318 \times 5.4067} = 1187.603 \; MPa$$

Elliptical contact surface dimensions as well as contact pressure for two different wheels in normal loading conditions are also described in Table 4.

In cases where flange contact occurs, the radius of contact body is different from normal contact. Beside that in the Hertz method, one point contact is assumed, therefore, only the results of case 1 can be validated by Hertz theory [21]. As illustrated in Table 4, the value of contact area is in the order of $1 \; cm^2$ which is much smaller than wheel and rail dimension [22].

Table 4. Comparison of the calculation results based on Hertz theory

wheel	Hertz Theory			
R_{11}	a (mm)	b (mm)	area (mm^2)	σ (MPa)
500	6.9052	5.4648	118.5496	1162.4872
460	6.8318	5.4067	116.0425	1187.603

4.1. Results and discussions

The fundamental step in this study is to investigate the contact area, the stress and pressure applied to it. A comparative analysis of equivalent stresses and contact pressures in different cases can lead to finding the most compatible combination of wheel and rail.

Table 5 shows the comparison of Von-Mises stress for six pairs of wheel and rail over three cases of loading conditions. As can be seen, in the case of normal contact, the maximum Von-mises stress reached 375MPa in wheel II-rail UIC60 interaction. According to the obtained stress values, wheel III-UIC60 rail matching shows better performance in passing straight track and curving while Von-Mises stress of wheel I-UIC60 is minimal in the case of crossing.

As can be seen in Table 6, there is satisfactory agreement between results obtained from FE simulation and Hertz theory. (Apart from the slight discrepancy, the results of contact pressure are confirmation of Hertz theory.)

Table 5. Comparison of the maximum values of Von-Mises Stress (MPa) obtained from FE simulation

	Case 1	Case 2	Case 3
Wheel I/ Rail UIC60	322.0	370.3	320.2
Wheel II/ Rail UIC60	375.0	366.7	385.0
Wheel III/ Rail UIC60	300.0	337.5	356.3
Wheel I/ Rail U33	366.7	375.0	382.0
Wheel II/ Rail U33	347.3	381.9	420.1
Wheel III/ Rail U33	343.8	377.5	356.3

Table 6. Contact Pressure (MPa) calculation from FE simulation and Hertz theory

		FEM		Hertz
	Radius	Rail UIC60	Rail U33	
Wheel I	460 mm	1293	1192	1187.6030
Wheel II	500 mm	1238	1142	1162.4872
Wheel III	460 mm	1192	1121	1187.6030

The comparison results of contact pressure and loading conditions are shown in Table 7. It can be seen, in the case of normal contact, the contact pressure of wheel III/ rail U33 is minimal. In the case of curving and crossing, wheel III and wheel I in contact with rail UIC60 represent the lowest values respectively.

Table 7. Comparison of the maximum values of Contact Pressure (MPa) obtained from FE simulation.

		Case 1	Case 2	Case 3
Rail UIC60	Wheel I	1293	1250	1238
	Wheel II	1238	1260	1274
	Wheel III	1192	1238	1274
Rail U33	Wheel I	1192	1375	1417
	Wheel II	1142	1429	1375
	Wheel III	1121	1282	1250

5. Conclusions

To study the conformity of different wheel and rail matchings, finite element models were used and then validated by Hertz theory. The influence of three cases, including straight track, curving, and crossing on contact parameters was established and the following results were achieved:

1- In the case of normal contact, the matching of wheel III/ Rail UIC60 shows the best performance. Its von-mises stress and contact pressure are minimal.

2- In the case of curving, the matching of wheel III/ Rail UIC60 has lower contact pressure and stress compared with other wheels and rails.

3- In the case of crossing, the matching of wheel I/ Rail UIC60 shows the most acceptable performance. The Von-Mises stress and contact pressure in this case represent the lowest values.

References

[1] S. Iwnicki, The Effect of Profiles on Wheel and Rail Damage. International Journal of Vehicle Structures & Systems, 1 (4), 99-104, (2009).

[2] Roger Enblom, Simulation of Wheel and Rail Profile Evolution-Wear Modelling and Validation, Licentiate Thesis, Royal Institute of Technology (KTH). ISSN 1651-7660, (2004).

[3] A. Sladkowski and M. Sitarz, Analysis of wheel–rail interaction using FE software. Wear. 258(7-8), 1217-1223, (2005).

[4] S. Iwnicki, Y. Chunlei, L. Fu and H. Yunhua, Influence of a vertical suspension on the dynamic behavior of heavy - duty truck wheel and rail. Journal of Southwest Jiaotong University, 46 (5), 820-825, (2010).

[5] J. Auciello, M. Ignesti, L. Marini and E. Meli. Development of a model for the analysis of wheel wear in railway vehicles. Meccanica ,48, 681-697, (2013).

[6] N. Wu and J. Zeng, Parametric analysis of wheel wear in high-speed vehicles, J. Mod. Transport. 22(2), 76–83, (2014).

[7] J. Liu, J. Zhang, X. Liu, H. Zhu, L. Zhang, and W. Shang, Wheel-rail profile matching based on finite element method for Beijing metro. IOP Conference Series: Materials Science and Engineering. vol. 231, (2017).

[8] İ. Esen and M. Eroğlu, 3D Finite element analysis of UIC 60 rail and UIC 515 wheel rolling contact and understanding starting mechanism of wear, 2nd International Iron and Steel Symposium (IISS'15), (2015).

[9] Y. Özdemir and P. Voltr, Analysis of the wheel and rail frictionless normal contact considering material parameters. Journal of Applied Mathematics and Computational Mechanics. 15. 101-109, (2016).

[10] P. Gurubarana, M. Afendia, I. Haftirman and K. Nanthini, Three-Dimensional Finite Element Analysis of Rolling Contact between Wheel and Rail. Int. J. Vehicle Structures & Systems, 9(3), 186-189, (2017).

[11] S. Sharma and A. Kumar, Dynamics Analysis of Wheel Rail Contact Using FEA. Procedia Engineering. 144. 1119-1128, (2016).

[12] T. Lack and J. Gerlici, Contact Area and Normal Stress Determination on Railway Wheel/ Rail Contact, Scientific Letters of the University of Zilina, vol 7, 38-45, (2005).

[13] J. Srivastava, P. Sarkar and V. Ranjan, Contact Stress Analysis in Wheel–Rail by Hertzian Method and Finite Element Method. Journal of The Institution of Engineers (India): Series C. 95. 319-325, (2014).

[14] A. Sladkowski and M. Sitarz. Analysis of wheel–rail interaction using FE software. Wear 258, 1217–1223, (2005).

[15] BS EN 13674-1:2011+A1:2017, Railway applications — Track — Rail Part 1: Vignole railway rails 46 kg/m and above.

[16] BS EN 13262:2004 +A2:2011, Railway applications — Wheelsets and bogies — Wheels — Product requirements.

[17] S. Iwnicki, A Handbook of Railway Vehicle Dynamics. CRC Press. First Ed, (2006).

[18] EN 13979-1:2003, Railway applications - Wheelsets and bogies - Monobloc Wheels - Technical approval procedure - Part 1: Forged and rolled wheels.

[19] El-sayed HM et al, Prediction of fatigue crack initiation life in railheads using finite element analysis. Ain Shams Eng J, 9(4), 2329-2342, (2017).

[20] Y. Liu, L. Liu and S. Mahadevan, Analysis of subsurface crack propagation under rolling contact loading in railroad wheels using FEM, Engineering Fracture Mechanics, 74, 2659-2674, (2007).

[21] R. Lewis and U. Olofsson, Basic tribology of the wheel-rail contact. Wheel-rail interface handbook, Woodhead Publishing Limited, Cambridge, pp 34–57, (2009).

[22] H. A. Otorabad, P. Hosseini Tehrani and D. Younesian, 3D transient elasto-plastic finite element analysis of a flatted railway wheel in rolling contact. Mechanics Based Design of Structures and Machines, 46(6), 751-766, (2018).

[23] U. Sellgren, T. Telliskivi, U. Olofsson and P. Kruse, A tool and a method for FE analysis of wheel and rail interaction, Proceedings of the International ANSYS Conference, Pittsburgh, (2000).

[24] S. Soemantri, W. Puja, B. Budiwantoro, M. Parwata and D. J. Schipper, Solution to Hertzian Contact Problem between Wheel and Rail for Small Radius of Curvature. Journal of Solid Mechanics and Materials Engineering, 4(6), 669-677, (2010).